SAE AERO DESIGN REPORT

Northern Arizona University

AeroJacks Team #316

Chazz Coppa

Matthew Espinoza

Jayden Glaus

Colton Tutrone

Tesla Ventsam

2024-2025

Certification of Qualification

Team Name	AeroJacks
Team Number	316
School	Northern Arizona University
Faculty Advisor	David Willy
Faculty Advisor's Email	David.Willy@nau.edu

Statement of Compliance

As faculty Adviser:

DW (Initial) I certify that the registered team members are enrolled in collegiate courses.

DW (Initial) I certify that this team has designed and constructed the radio-controlled aircraft in the past nine (9) months with the intention to use this aircraft in the **2025** SAE Aero Design competition, without direct assistance from professional engineers, R/C model experts, and/or related professionals.

DW (Initial) I certify that this year's Design Report has original content written by members of this year's team.

DW (Initial) I certify that all reused content has been properly referenced and is in compliance with the University's plagiarism and reuse policies.

DW (Initial) I certify that the team shall use the Requirements Check & Safety and Airworthiness Inspection checklists to inspect their aircraft before arrival at Technical Inspection and that the team shall submit the completed checklists, signed by the Faculty Advisor or Team Captain, to the inspectors before Technical Inspection begins.

Signature of Faculty Advisor — Date: 02/15/2025

Signature of Team Captain — Date: 02/15/2025

Note: **A copy of this statement needs to be included in your Design Report as page 2 (Reference Section 4.3)**

Table of Contents

1.0 Executive Summary

This document outlines the processes the Northern Arizona University team used to design and manufacture a remote-controlled (RC) aircraft for the Society of Automotive Engineers (SAE) Aero Design West 2025 micro competition. The methodology, overall design, analysis, performance, and manufacturing process are all explained to build the aircraft. The main goal of the project is to build a lightweight plane that can transport 67 fluid ounces of water. The current design can transport 67 fluid ounces and has been optimized within the SAE design requirements.

1.1 System Overview

The aircraft is a monoplane with a blended wing body. To keep a lightweight design, the fuselage has a truss structure and was laser-cut from pine wood with a tricycle, front-steering landing gear. The propulsion system is a tractor configuration RC motor with a single three blade propeller. The wings and stabilizers are made of balsa, laser-cut ribs of a clark-y airfoil with two 3.1x3.1” carbon fiber spars, balsa wood leading and trailing edges, and wrapped in shrink wrap. This airfoil was chosen to maximize lift with an angle of attack of fifteen degrees. The electric circuit has a 450 Watt power limiter and a red arming plug. Figure 1 displays the final design of the aircraft.

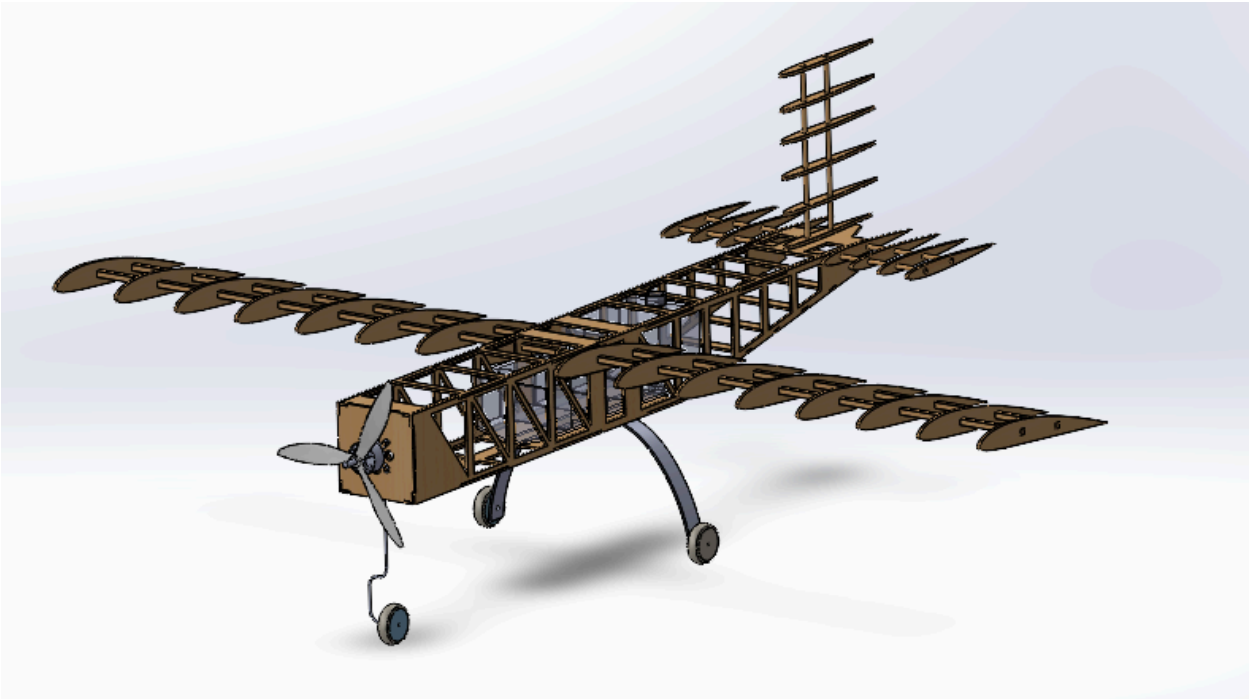

Figure 1: AeroJacks Final Design

1.2 Discriminators

The fuselage provides a light-weight design, as unnecessary materials and weight are removed from the aircraft. The use of pine and balsa wood also decrease the design's weight without losing durability. Laser-cutting each piece of the fuselage and spars allowed for precise, easily replicable manufacturing. The blended wing body provides added security to the wings, providing support in critical areas. The wings are located high on the body (nearing a high-wing configuration) which increases stability and enhances lift at low speeds. The tractor configuration of the propeller allows for better efficiency, as airflow is not disrupted by the fuselage. The front-mounted engine also provides a natural shift forward of the center of gravity and improves stability.

2.0 Schedule Summary

The team started working on this project in September 2024. The first four months of the process focused on research and prototype development. Each team member completed preliminary research on the overall components of an RC airplane, then researched specific subsystems such as the wings, fuselage, horizontal and vertical stabilizers, thrust, landing gear, and electronic system. After completing research the team worked on designing prototype airplanes, then refining and optimizing the early designs to become competition ready for April 2025. Figures 2 and 3 display the fall and spring Gantt Charts of the team schedule. The fall schedule focused on initial research, beginning iterative plane designs, and completing calculations for the goal takeoff speed and plane dimensions. Once these designs were known, iterative designing and testing began. The spring schedule focused on finalization and construction of the aircraft design.

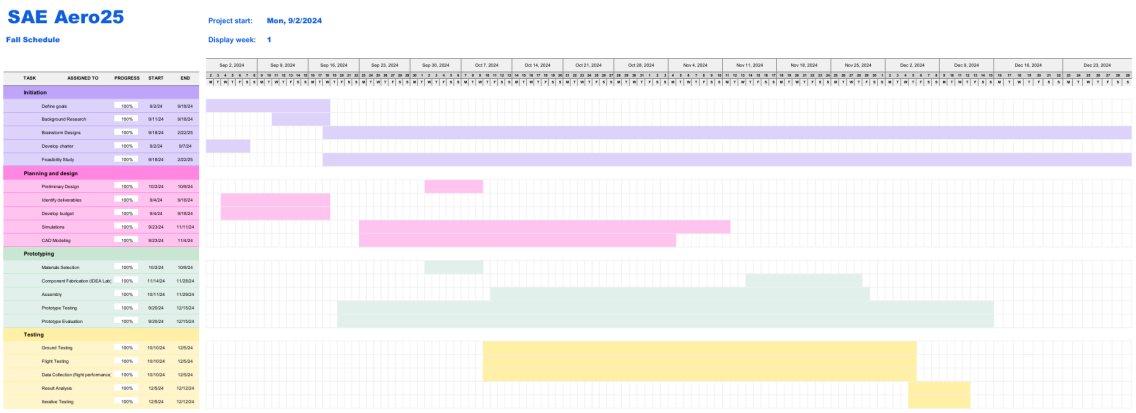

Figure 2: AeroJacks Fall Schedule Gantt Chart

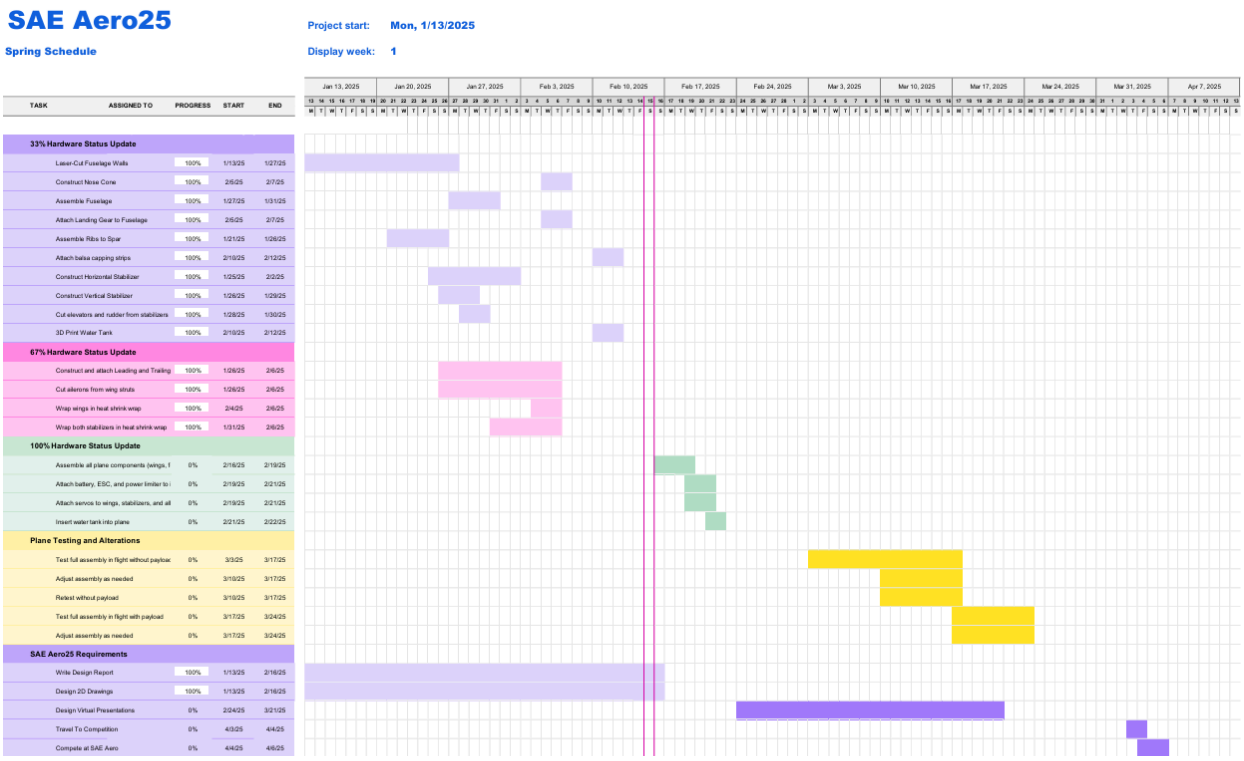

Figure 3: AeroJacks Spring Schedule Gantt Chart

3.0 Design Layout & Trades

When starting the design process, the team created a functional decomposition to better understand the inputs and outputs of the aircraft system. This was created with the researched knowledge of RC airplanes and broken down into the base steps for plane control. Figure 4 shows the team's functional decomposition.

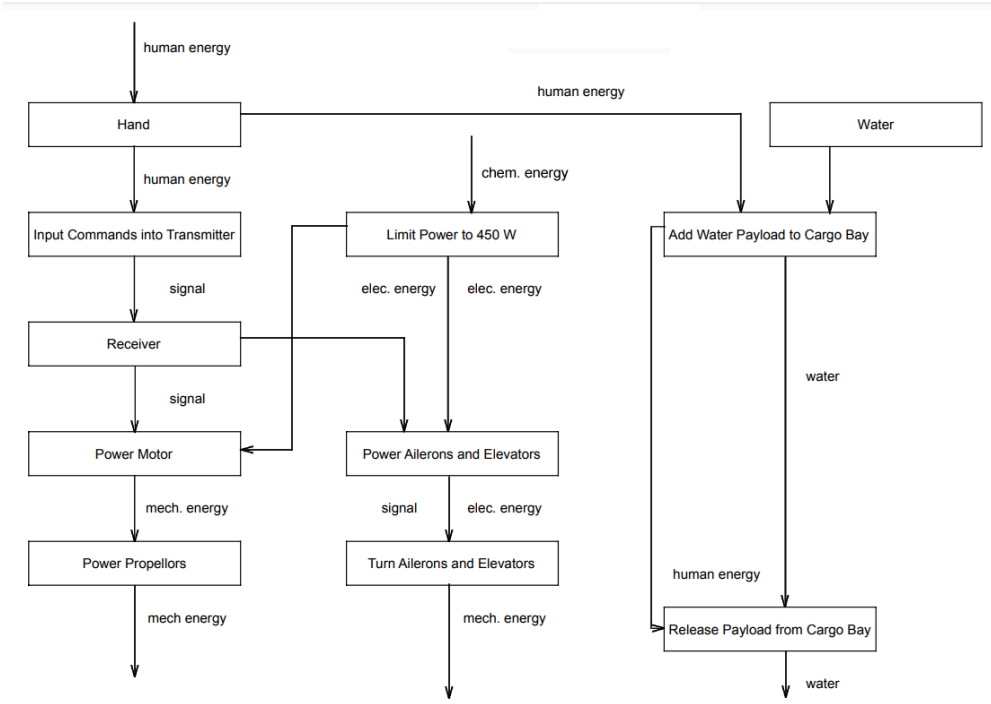

Figure 4: Functional Decomposition

The team also created an electrical diagram in order to understand each aspect of the plane's control system and power. The electrical diagram is shown in Figure 5. After deciding the foundational requirements of the plane, the team moved forward with iterative design.

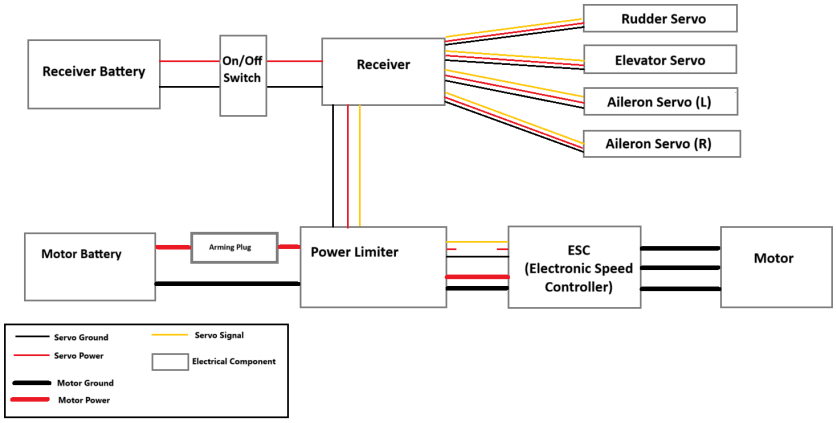

Figure 5: Electrical Diagram

3.1 Overall Design Layout and Size

The dimensions of the aircraft can be seen in **Table 1.**

Table 1: Plane Dimensions

Component	**Dimension**
Wingspan	54.0 inches
Chord Length	11.0 inches
Wing Area	594.0 inches^2
Airfoil	Clark Y
Propellor Size	Master Airscrew 13 x 8 inch
Landing Gear	12.59 inches (width) 6.29 inches (height) 1.10 inches (depth)
Nose to Tail Length	41 inches

3.2 Optimization

A MATLAB code was created to optimize the dimensions of the plane. Initial parameters were first set as a starting point, being the wing, horizontal tail, and vertical tail dimensions (including the airfoil, the maximum angle of attack, wing density, half-span, root chord, taper ratio, aspect ratio, and more), the fuselage dimensions (the length, width, height, and density of the fuselage), and the payload parameters. Some dimensions were set to be unchanging, such as the density of materials used and the payload parameters, then the code was run with the goal of optimizing the score shown in equation 1, which was the scoring equation for the competition.

$$Final\ Flight\ Score\ =\ 3\ *\ W_{payload}\ *\ M\ +\ Z \tag{1}$$

$$M\ =\ \frac{11}{(W_{empty}-1)^4+8.9} \tag{2}$$

$$Z = B_{takeoff} - S^{1.5} \quad (3)$$

$W_{payload} = Payload\ Weight\ (lbs)$

$W_{empty} = Empty\ Weight\ (lbs)$

$S = Wingspan\ (ft)$

$$B_{takeoff} = \begin{cases} 20 & 0 \leq x \leq 20\ ft \\ 15 & 10 < x \leq 25\ ft \\ 9 & 25 < x \leq 50\ ft \\ 0 & 50 < x \leq 100\ ft \end{cases}$$

The code analyzed possible scores and depicted the score optimization. The parameters with the highest output score were then presented in code and used in the team design.

3.3 Design Features and Details (Subassembly Sizing)

SAE Aero25 aircraft subassemblies were structured based on strength, weight limit, and aerodynamic efficiency. All of the components were clearly laid out to offer optimal performance in competitive environments while achieving strength versus light-weight construction balance. The fuselage is structured to accommodate the payload water tank without affecting its aerodynamic shape and therefore minimal drag. Laser-cut plywood panels supported by metal brackets are primarily employed to construct it. The design achieves maximum balance between strength and lightness, with sufficient structural support without excessive weight. Pre-drilled slots were made available for the attachment of electronics, the motor, and landing gear. The fuselage structure was also strengthened in high-stress areas to prevent deflection under load.

Additional bracing was incorporated at subassembly connection points to offer structural integrity during flight and landing.

The wingspan is 54 inches with 11-inch ribs to provide maximum lift while maintaining an efficient scoring size. The structure is constructed from balsa wood ribs, a carbon fiber wing spar, and shrink wrap covering to achieve a light yet resilient surface. A 2-inch control surface was incorporated to enhance maneuverability. Design for the wing involved iterations with designs aiming at maximum aerodynamic efficiency, minimum structure weight, and the ease of assembling. Wing attach method was purposely chosen for permitting rapid as well as rigid fixing so the flight loads are not weakening the structure.

The tail assembly comprises a horizontal stabilizer and a vertical stabilizer, each with a control surface (the rudder and the elevator). The control surfaces are a hinged elevator and rudder with smooth motion, operated through servo systems. For greater stability of flight, the attachment points of the tail assembly were reinforced with wood glue and metal hardware, reducing misalignment at high-speed flight. The horizontal stabilizer is made up of balsa ribs and spruce spars. The control surfaces consist of a hinged elevator and rudder, with accurate movement, controlled through servo mechanisms. For increased stability during flight, the tail assembly mounting points were reinforced to reduce the likelihood of misalignment during high-speed flight.

The water tank is 67 fl oz in capacity and is constructed to evenly distribute weight inside the fuselage. It is 3D-printed from PLA with a waterproof treatment to avoid leakage. The mounting system has a reinforced cradle to secure the tank to avoid movement during flight. Particular attention was paid to where the tank would be placed so that its center of gravity is optimal under varying flight conditions

4.0 Loads and Environments, Assumptions

The following subsections details the various loads that the aircraft will experience. The loads that have the greatest impact on the plane are the takeoff, landing, and payload loads. While loads on the aircraft are important to analyze, the environmental conditions need to be considered to provide the team with a general idea of how the plane will fly.

4.1 Design Loads

High aerodynamic loads are encountered during takeoff due to increased angles of attack. The wings and fuselage must withstand lift and drag forces as the plane accelerates to achieve takeoff. Landing generates significant forces on the fuselage and landing gear. These forces are analyzed to ensure durability and survivability during hard landings. The water payload induces additional weight, affecting wing bending moments and fuselage stresses. Structural reinforcement ensures safe operation under full and partial payload conditions.

4.2 Environmental Conditions

The competition is being held in Van Nuys California, where weather conditions differ to Flagstaff Arizona. The team collected data from historical atmospheric conditions to obtain average temperature, pressure, and density for a comparison of Reynolds numbers between Van Nuys and Flagstaff.

Table 2: Parameters and Reynolds Numbers

	μ (slug/ft.s)	V (ft/s)	ρ (slug/ft^3)	P (psi)	T (F)	Re
Sea Level	3.74E-07	49.2	0.00237	14.7	60	286524.27
Van Nuys	3.75E-07	49.2	0.00234	14.73	62	280729.53
Flagstaff	3.68E-07	49.2	0.00204	14.68	49	249677.24

To calculate Reynolds number, the above parameters are used in equation 4 below.

$$Re = \frac{\rho V l}{\mu} \tag{4}$$

Where V is the velocity, l is the characteristic length, ρ is the fluid density, and μ is the absolute viscosity coefficient. The viscosity is determined using Sutherland's equation (equation 5):

$$\frac{\mu}{\mu_0} = \left(\frac{T}{T_0}\right)^{\frac{3}{2}} \left(\frac{T_0+S}{T+S}\right) \tag{5}$$

where T is the temperature, T_0 is the reference temperature at sea level, μ_0 is the absolute viscosity at sea level, and S is the Sutherland constant.

5.0 Analysis

The analysis of the plane structure, design, and aerodynamic properties were done primarily in computer software programs. The software programs included XFLR5, MATLab, and SOLIDWorks. The team performed various analyses to maximize the theoretical performance of the plane as well as to maximize the score received during competition. The primary focus of the analyses were to ensure that the plane could meet the competition specified payload requirements and have the smallest wingspan possible. The various software programs allowed for an iterative design process which made changing small details simpler and easier.

5.1 Analysis Techniques

The analysis techniques used during the design of this plane were an optimization program using MATLab, a flow simulation and 3D model in SOLIDWorks, ANSYS, and Pradtl's lifting line theory and the 3D panel method in XFLR5. Using the optimization code, a starting point for dimensions of the wings and fuselage could be conducted. The code used the competition rules as a way to maximize the points received. The flow simulation in SOLIDWorks was used to see forces acting on the fuselage due to airflow. The most extensive analyses were done using XFLR5. The lifting line theory and the 3D panel method were already built into XFLR5. Using both techniques, the coefficient of lift and drag were calculated according to the airfoil and wing shape. ANSYS, provided a method to complete a finite element analysis on the plane wings. ANSYS used the imported SOLIDWORKS CAD model of the wings and after setting the materials and forces the wings endured, a finite element analysis was completed.

5.1.1 Developed Models

Figures 6 and 7 are the products of the XFLR5 calculations. Using the coefficients of lift and drag generated by the software, a graphical representation can be shown for both lift and drag of the designed wing. The wing was set at a permanent angle of attack based on these graphs. The chosen angle is +7°. This was done to get the most lift without inducing an unacceptable amount of drag.

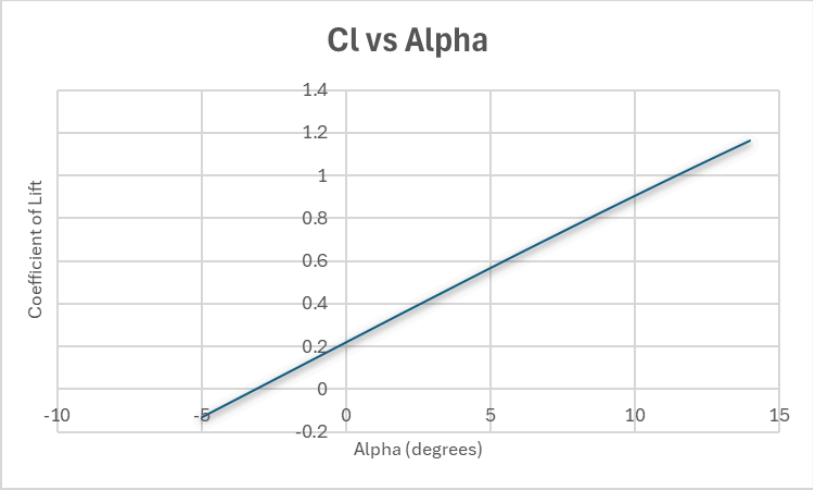

Figure 6: Coefficient of Lift versus Angle of Attack

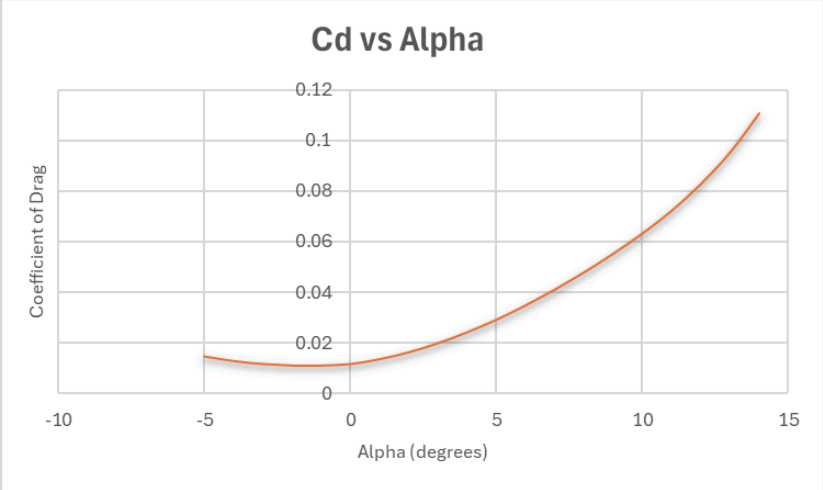

Figure 7: Coefficient of Drag versus Angle of Attack

5.2 Performance Analysis

The performance analysis that was conducted was a lift versus velocity analysis. Using the data collected from the XFLR5 software the coefficients of lift and drag were calculated and then were plugged into the lift and drag equations.

$$L = \frac{1}{2}\rho v^2 C_L S \quad (6)$$

L = Lift
ρ = Air Density
v = Velocity
S = Wing Area
C_L = Lift Coefficient

$$D = \frac{1}{2} v^2 C_D S \quad (7)$$

D = Drag
C_D = Drag Coefficient

From these equations, a model to predict the needed velocity to get a certain lift could be created. This was used to predict payload capacity and takeoff velocity and are shown in section 5.2.1.

5.2.1 Takeoff Performance

Figures 8 and 9 show the lift and drag at various velocities. The method was that in order to lift a certain amount of weight, then the plane needs to move at a certain speed. The plane was initially estimated to be around 35N (7.86 lbs) in weight. Given this, the speed necessary to lift this weight can be seen. The graph depicting drag as a function of velocity was used to see how much drag would be acting on the aircraft at its takeoff speed.

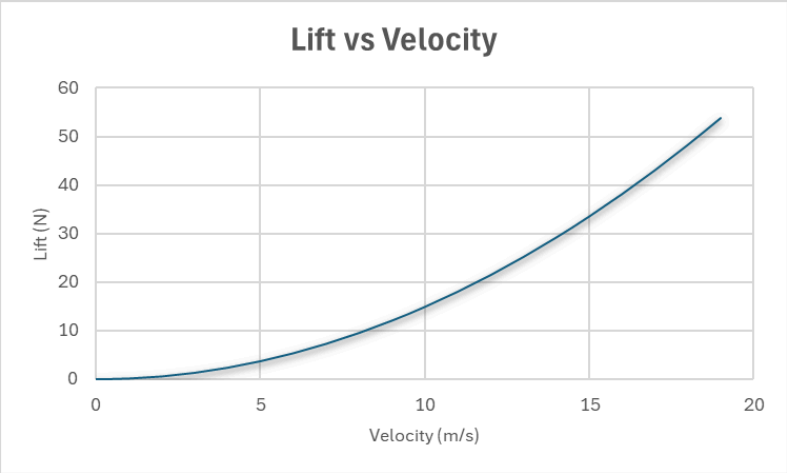

Figure 8: Lift [N] versus Velocity [m/s]

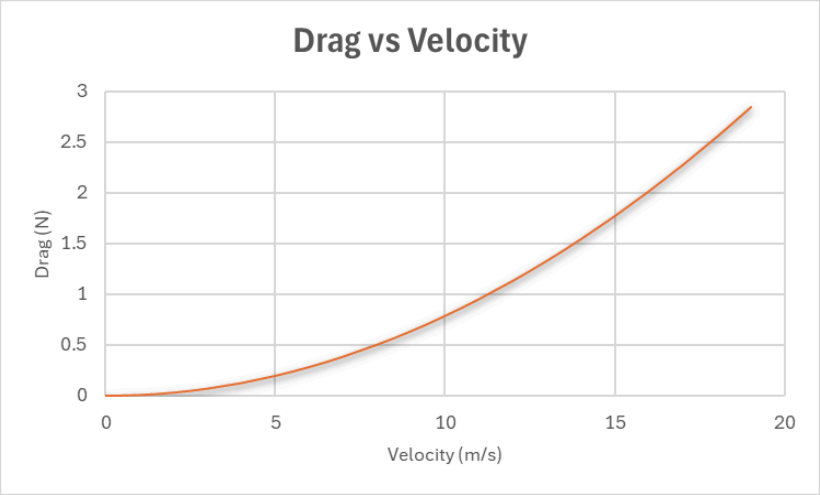

Figure 9: Drag [N] versus Velocity [m/s]

5.2.2 Payload Prediction

Similar to predicting maximum takeoff weight, figure 8 can be used to predict the payload that can be carried depending on the airspeed. The velocity on the graph represents the speed of the air and not the speed of the wing. From this, it can be seen that if headwinds are strong enough, the plane can exceed its normal takeoff weight prediction of 35N (including full payload) and perform well while under around 10-20N more load than expected.

5.3 Structural Analysis

A structural analysis of both the wings and fuselage were performed to ensure the design would be able to withstand the forces that they will be subjected to. The stress across the wings/fuselage and maximum stress points were calculated using SOLIDWorks. These values were critical to ensuring a safe design.

5.3.1 Wing Analysis

To simplify the analysis, half of the wing is demonstrated as a beam shown in figure 10, with a maximum lift force of 20 lbf. The wing experiences a maximum stress of 4.734 kpsi on the back

spar with a minimum factor of safety of 1.689. To replicate the strength of carbon fiber, 6061 aluminum alloy was used in place for the spars. The wing experiences 0.039 inches of displacement and has the most strain at the max stress point shown in figure 11.

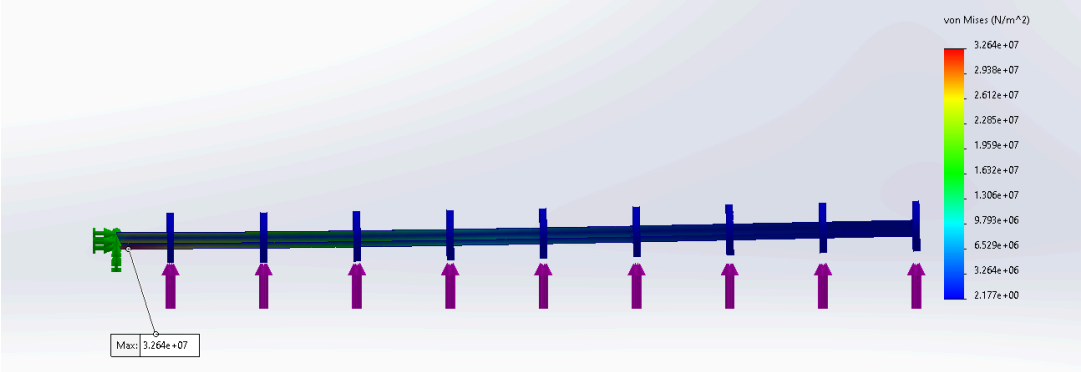

Figure 10: Stress analysis of wing

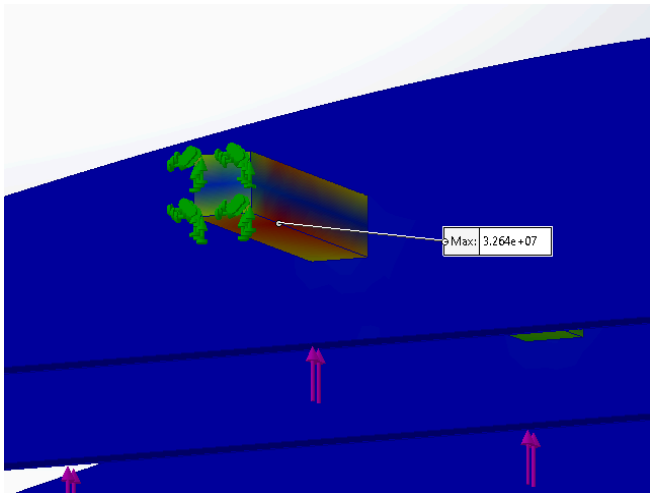

Figure 11: Wing's Max Stress Point

5.3.2 Fuselage Analysis

The fuselage is primarily made of balsa wood and withstands aerodynamic and payload loads. It experiences a maximum stress of 1.158 kpsi with a minimum factor of safety of 2.503. Figure 12 shows a displacement of 0.291 inches and experiences the most strain at the max stress point shown in figure 13.

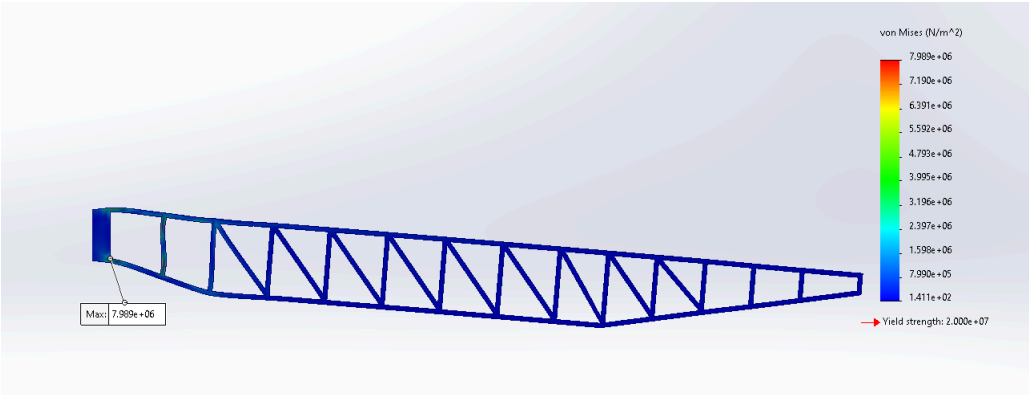

Figure 12: Fuselage Stress Analysis

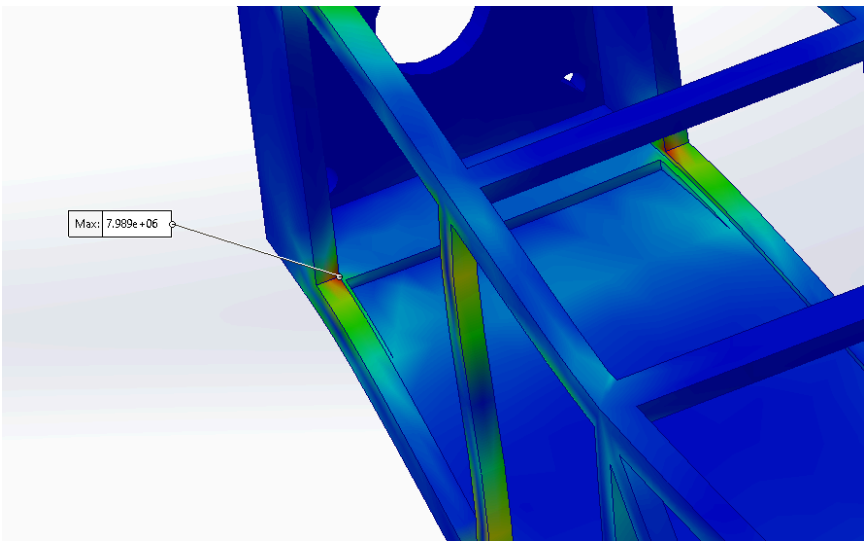

Figure 13: Fuselage's Max Stress Point

6.0 Assembly & Sub-Assembly, Test and Integration

This section outlines assembly, integration, and testing procedures for structural integrity, performance, and safety. The aircraft is made of carbon fiber, balsa wood, light plywood, and 3D-printed PETG components, prioritizing weight, efficiency, and durability

6.1 Wing Assembly and Integration

The wings feature 5/16 inch square pultruded carbon fiber spars, 1/8-inch laser-cut balsa ribs, and balsa leading and trailing edges. The ribs are held in a form while they are glued to the spars. Once bonded to the spar and edges, the ribs are covered with 1/16-inch balsa sheeting and Monokote for aerodynamics. Both wing halves slide through the fuselage and are clamped together for easy disassembly and transport.

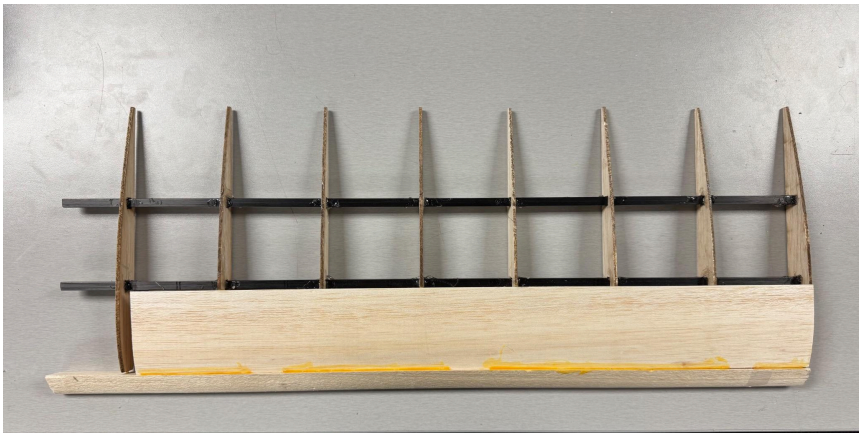

Figure 14: Partially constructed wing

6.2 Fuselage and Tail Integration

The fuselage is made of 1/8-inch laser-cut plywood with interlocking joints and metal braces. The 3D-printed PETG water tank is securely mounted inside for stability. The horizontal and vertical stabilizers are constructed similarly to the wings but with wooden dowel spars.

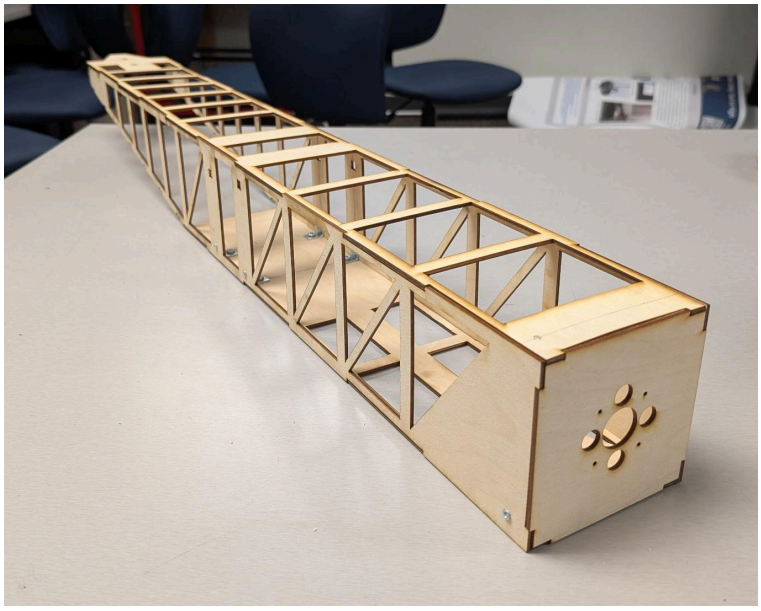

Figure 15: Partially assembled fuselage

6.3 Landing Gear and Control System

The steerable front wheel links to the rudder controls for ground maneuverability, while lightweight carbon fiber struts make up the rear landing gear. Independent battery systems provide reliable power for propulsion and avionics.

6.4 Testing and Validation

6.4.1 Structural and Load Testing

Static load testing verified the carbon fiber spars' ability to distribute aerodynamic forces without deformation. Ground tests confirmed the landing gear's durability and responsiveness.

6.4.2 Control Surface Calibration

The control surfaces were tested for full range of motion and adequate servo response time. All mechanical linkages were checked for reliable performance.

6.4.3 Electrical System and Thrust Testing

Extensive circuit testing was conducted to ensure the proper operation of the motor, batteries, and propellers. Thrust stand tests were performed using various motors, propellers, and batteries. The maximum thrust achieved was approximately 2,400 grams at an altitude of 7,000 feet above sea level. The calculated thrust at the competition altitude is expected to be around 2,800 grams.

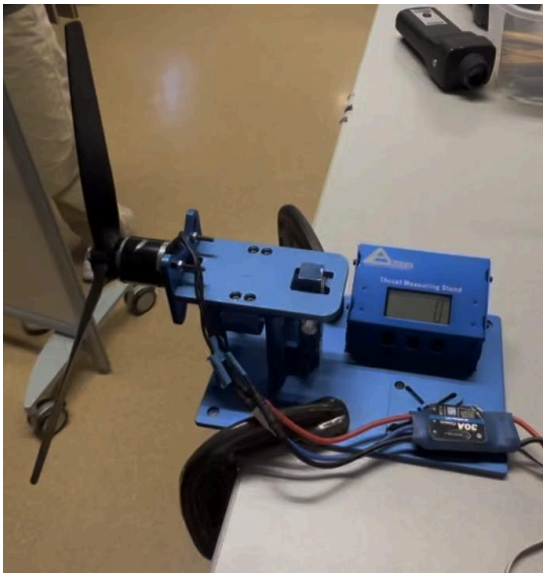

Figure 16: Thrust measuring stand

7.0 Manufacturing

The manufacturing process followed a systematic approach for accuracy and speed. Each component was built using specialized techniques to provide accuracy and consistency, minimizing wastage of material.

The fuselage was built using precision laser-cut plywood panels designed to interlock. Wood glue was applied to the critical joints and metal brackets were used at stress points for reinforcement. The motor mount was a bespoke plywood bracket that securely fastened the motor at the front of the fuselage. In addition, structural reinforcements were added at high-stress

junctions to prevent warping under long-term loading. Assembly was meticulously planned to be systematic to ensure alignment and minimize potential errors.

The wings were constructed from laser-cut balsa wood ribs, which were laid along carbon fiber spars. Prefabricated leading and trailing edges were fitted into the ribs to provide structural strength. Heat-treated shrink wrap was applied to provide an aerodynamic surface with minimum weight and yet be strong. Attention was taken to maintain uniform rib spacing to ensure that aerodynamic forces would be evenly distributed across the wing surface. Additional tests were carried out to examine the strength of the wing under simulated flight loading.

The tail assembly was constructed from pre-cut balsa wood ribs and spars and was cemented into the fuselage for a solid and permanent bond. The rudder and elevator were fitted with hinge mechanisms for attachment and were connected to servo motors for precise control. Guides were used during assembly to ensure correct positioning of the control surfaces. Mechanical testing was done to ensure that the hinge attachments had free and smooth movement under load. Alignment guides were used during assembly to ensure proper alignment of the control surfaces. Mechanical testing was done to ensure that the hinge attachments had free and smooth movement under load.

The water tank was 3D printed using PLA filament and reinforced in stress-prone areas. It was sealed using a waterproofing sealant and underwent leak testing for durability. The tank was attached within the fuselage using a custom-designed bracket to maintain center-of-mass balance.

Final aircraft assembly involved integrating the fuselage, wings, and tail using dedicated mounting points. Motor, receiver, battery, and servos were wired and tested for proper

functionality. Control surfaces were calibrated and center of gravity was checked prior to flight testing. Additional weight distribution tests were conducted to verify that the handling qualities of the aircraft were as anticipated in design. The completed assembly was subjected to a series of ground-based tests to assess the structural integrity and responsiveness of control mechanisms. This systematic approach ensured that subassemblies were all built and assembled with precision, optimizing the performance for SAE Aero25 competition. Combining thorough testing, precise manufacturing, and material selection strategy created an aircraft design that not only wowed competition specifications but also engineering best practices.

8.0 Conclusion

The NAU Aero Jacks aircraft has gone through many iterations of design, analysis, and testing. The plane features a high wing blended body design with a laser cut fuselage and laser cut wing and tail ribs. The water tank was 3D printed with baffles on the inside for payload oscillation damping. The design of the RC plane is designed to optimize stability while decreasing design weight. The plane is projected to have a stable flight in competition and efficiently deliver the 67 ounce water payload.

9.0 References

[1] Model, “Model Aircraft Design Optimization with MATLAB,” YouTube, Dec. 13, 2022. https://youtu.be/ipjsxi04euA?si=2-yd1c7OWuIMlSOz (accessed Oct. 04, 2024).

[2] SAE Aero Design - Rules" "SAE Aero Design - Rules," SAE Aero Design, https://www.saeaerodesign.com/cdsweb/gen/DocumentResources.aspx.

[3] J. D. Anderson, “Aircraft Performance and Design”. Boston, Mass. Mcgraw-Hill Higher Education, 2012.

[4] Daniel P. Raymer “Aircraft Design-A Conceptual Approach”, American Institute of

Aeronautics and Astronautics

[5] J. D. Anderson, Fundamentals of Aerodynamics, 6th ed., New York, NY: McGraw-Hill Education, 2017

[6] Kroo, “Drag Due to Lift: Concepts for Prediction and Reduction,” Annual Review of Fluid Mechanics, vol. 33, pp. 587-617, 2001. doi: 10.1146/annurev.fluid.33.1.587.

[7] OpenVSP (Version 3.40.1) [Software]. (2023) National Aeronautics and Space Administration. https://openvsp.org/

[8] SAE University Programs. “SAE Aero Design”, Youtube, Sept 5, 2024. [57 Video Viles]. Available: https://youtu.be/TH40KCVfFkQ?si=AvlQY_qM_U-qS5uI

[9] N. Harris, “Static stability and control derivatives for light aircraft,” AIAA Journal of Aircraft, vol. 45, no. 3, pp. 845–857, 2008.

[10] E. Torenbeek, “Estimating the aerodynamic center and static margin for conceptual aircraft design,” Aerospace Science and Technology, vol. 12, no. 4, pp. 289–296, 2008.

Appendix A - Technical Data Sheet

Team Name: Aero Jacks

School Name: Northern Arizona University

Team Number: 316

The figures below show the plots of the neutral point and center of gravity versus the angle of attack and the static margin versus the angle of attack. The center of gravity shifts further back from the neutral point as the angle of attack increases, as the water's center of gravity will slightly shift as the angle increases as well. There is not a large change, as the water tank includes baffles to decrease the center of gravity shift and dampen oscillations in the water during flight. The minimum static margin is 2.23% and the maximum is 3.01%. Given the low static margin, the plane will require small control inputs due to higher maneuverability.

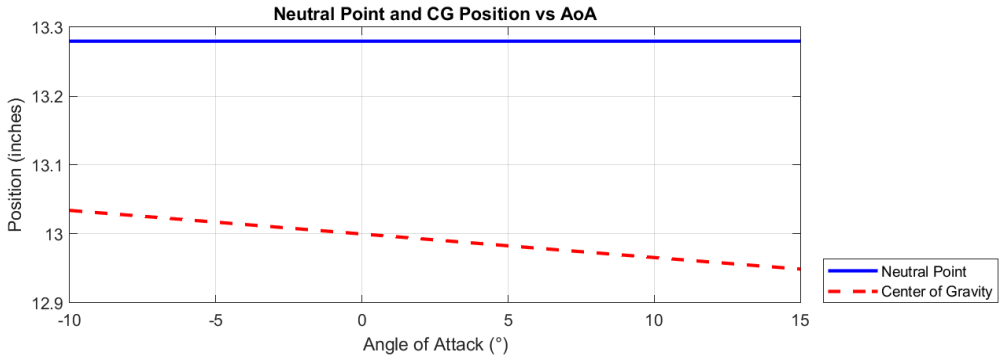

Figure 17: Neutral Point and Center of Gravity Positions (inches) versus Angle of Attack (°)

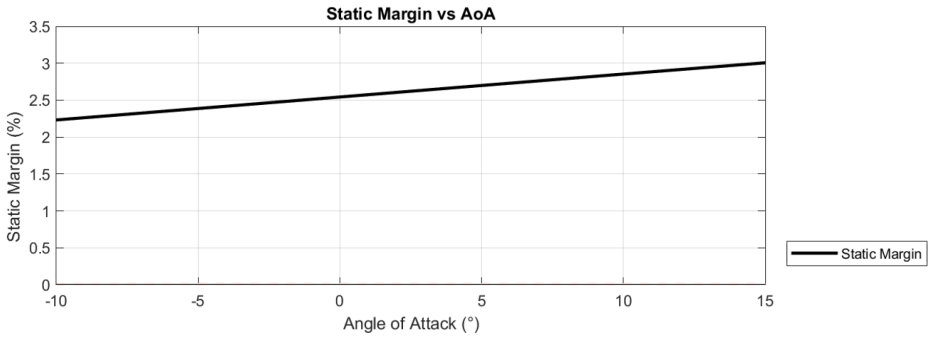

Figure 18: Static Margin (%)

Appendix B - 2D Drawing